Microwave Studies of a Pulsed Glow Discharge

C. W. DAVIDSON* AND W. E. J. FARVIS
Electrical Engineering Department, University of Edinburgh, Edinburgh, Scotland
(Received April 30, 1962)

An investigation of the behavior of a pulsed glow discharge in helium has been made using a microwave method (3 Gc/sec) supplemented by light intensity and spectroscopic measurements. The discharge tube was mounted across a section of rectangular waveguide, parallel to the electric field vector of the TE_{10} mode. Time-resolved microwave admittance measurements and dielectric post theory were used to determine the variation in parameters for the section of the discharge within the waveguide. The method is particularly suitable for high electron densities and resolutions of 1 cm along the axis of the discharge and 1 μsec in time can be obtained without difficulty. The variation in discharge parameters was studied when rectangular current pulses of a few milliamperes were superimposed on a small dc maintaining current. A low-pulse repetition frequency was used and the admittance measurements were recorded photographically in order to minimize changes in discharge characteristics and to extend the useful life of the discharge tubes. Sufficient results have been obtained to give a qualitative picture of the behavior of a glow discharge under transient conditions, and a recombination coefficient for helium of approximately 10^{-8} cm^3/ion sec has been measured during the afterglow period. This is in good agreement with results obtained by other microwave methods.

1. INTRODUCTION

MICROWAVE techniques have been widely applied to the study of ionized gases in recent years. In many cases the discharge to be studied has been mounted in a resonant cavity and the discharge parameters have then been calculated from changes in the resonant frequency and microwave losses of the cavity.

An alternative method is to mount a discharge tube across a section of rectangular waveguide, parallel to the electric field vector of the TE_{10} mode, so that it behaves as a dielectric post. The discharge parameters can then be obtained from the microwave admittance of the discharge, measured with a normal standing-wave probe in the waveguide. This method appears to have received little attention, although Prime[1] applied it to the study of dc discharges in mercury vapor and Sekiguchi and Herndon[2] have used it in measurements of the thermal conductivity of an electron gas. The purpose of this paper is to describe the application of the dielectric post method and time-resolved microwave addmittance measurements to the study of transient discharges, with particular reference to the pulsed glow discharge.

The most convenient frequencies for measurements of this type are in S band (3 Gc/sec) and X band (10 Gc/sec), as equipment is readily available. S band was used, as the lower frequency leads to greater sensitivity and accuracy for electron densities of the order expected in glow discharges at pressures of a few millimeters of mercury.

As the dynamic impedance of a glow discharge may be low, or negative, under some conditions, the discharge was fed from a high-impedance source which generated rectangular current pulses of a few milliamperes superimposed on a dc maintaining current of approximately 250 μA. The resulting variation in electron density and collision frequency in the region of the discharge within the waveguide produced a time-varying standing-wave pattern in the waveguide. A photographic method was used to record this standing-wave pattern so that changes in discharge characteristics during the period of the measurements were negligible.

In order to study the variation of the parameters along the axis of the discharge, the discharge tube was mounted in a section of waveguide with a reduced height of 1 cm. The values of discharge parameters obtained using this technique are therefore averaged over the cross section of the discharge and the 1-cm length.

To establish the feasibility of the method and simplify the problem of interpreting the results the measurements were restricted to discharges in helium, which has already been studied using other microwave methods.

2. DIELECTRIC POST THEORY

Marcuvitz[3] has given expressions which relate the parameters of a T-equivalent circuit for a dielectric post in rectangular waveguide to the dielectric constant of the post. These expressions are valid for negative or complex relative dielectric constant $\epsilon_r=\epsilon_r'-j\epsilon_r''$, and for a central post of small diameter $(2R/a\ll 1)$ the equivalent circuit reduces to a simple normalized shunt admittance, $\mathbf{y}=g+jb$, given by

$$\frac{1}{\mathbf{y}}=-j\frac{a}{2\lambda_g}\left\{\frac{J_0(\beta)}{J_0(\alpha)}\times\frac{1}{\beta J_0(\alpha)J_1(\beta)-\alpha J_0(\beta)J_1(\alpha)}-S_0+\frac{\alpha^2}{4}\right\}, \quad (2.1)$$

* Present address: Nuclear Enterprises (G.B.) Ltd., Sighthill, Edinburgh, Scotland.

[1] H. A. Prime, Australian J. Sci. Research **A5**, 607 (1952).

[2] T. Sekiguchi and R. C. Herndon, Phys. Rev. **112**, 1 (1958).

[3] N. Marcuvitz, *Waveguide Handbook*, Radiation Laboratory Series No. 10 (McGraw-Hill Book Company, New York, 1951), p. 266.

where

$$S_0=\ln\left(\frac{4a}{2\pi R}\right)-2+2\sum_{\substack{n=3\\ n\text{ odd}}}^{\infty}\left\{\frac{1}{[n^2-(2a/\lambda)^2]^{\frac{1}{2}}}-\frac{1}{n}\right\},$$

$\alpha=2\pi R/\lambda$, $\beta=\alpha\varepsilon_r^{\frac{1}{2}}$, R is the radius of the post, a is the width of the waveguide, and the other symbols have the usual significance.

Anderson[4] has used an approximate form of this equation in a recent X-band study of a pulsed discharge in helium. The geometry of Anderson's apparatus was similar to that described here, but the waveguide system behaved as a resonant cavity.

Equation (2.1) can be rearranged to give

$$\beta\frac{J_1(\beta)}{J_0(\beta)}=\frac{1}{J_0^2(\alpha)}\frac{1}{(S_0-\alpha^2/4+j2\lambda_g/a\mathrm{y})}+\alpha\frac{J_1(\alpha)}{J_0(\alpha)}. \quad (2.2)$$

For $\alpha,\beta\ll 1$ the Bessel functions can be replaced by the first term of the series expansion, so that,

$$\beta^2/2=\alpha^2\varepsilon_r/2=1/(S_0-\alpha^2/4+j2\lambda_g/a\mathrm{y})+\tfrac{1}{2}\alpha^2. \quad (2.3)$$

In these experiments, the discharge was 7.5 mm in diameter in waveguide RG48/U at 3 Gc/sec. Substitution of the appropriate constants in Eq. (2.3) gives

$$(\varepsilon_r-1)=60\mathrm{y}/(\mathrm{y}+j6.25). \quad (2.4)$$

However, in this case $\alpha\doteqdot 0.24$, so that Eq. (2.4) is not valid even for $\varepsilon_r\sim 1$ and a more accurate solution of Eq. (2.2) is necessary.

The left-hand side of Eq. (2.2) is a function of β, where $\beta=l+jm$, say, and is in general complex. It can be expanded about l or m, whichever is the greater, to give a Taylor series involving only l,m and the ratio $J_1(l)/J_0(l)$ or $I_1(m)/I_0(m)$. The series converges rapidly for all reasonable values of l and m and it can be readily evaluated with the aid of a digital computer. Hence, for any value of ε_r the corresponding microwave admittance can be calculated.

Results obtained using a Ferranti-Pegasus computer are shown in Fig. 1. Comparison of these results with the approximate solution, Eq. (2.4), shows that the approximation may be in error by as much as 20% for the geometry used in these experiments.

3. RELATION BETWEEN THE DISCHARGE PARAMETERS AND THE MEASURED DIELECTRIC CONSTANT

The microwave dielectric constant of an ionized gas must be interpreted in terms of the discharge parameters, for example, the electron density N and the collision frequency ν.

In the classical solution of this problem the electron velocity is assumed to be harmonic in time with the applied microwave field and a collision frequency ν is

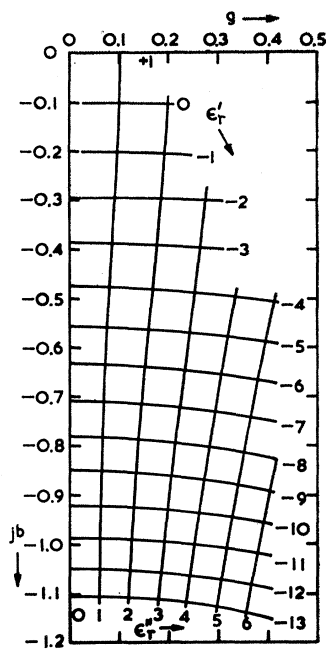

FIG. 1. Computed values of normalized microwave admittance, $\mathrm{y}=g+jb$, plotted as a function of complex dielectric constant, $\varepsilon_r=\epsilon_r'-j\epsilon_r''$.

introduced to account for losses due to collisions between electrons and gas molecules. This approach leads to the usual expression for the complex dielectric constant of an ionized gas:

$$\varepsilon_r=\epsilon_r'-\epsilon_r''=\left[1-\frac{Ne^2}{m\epsilon_0(\omega^2+\nu^2)}\right]-j\left[\frac{Ne^2\nu}{m\omega\epsilon_0(\omega^2+\nu^2)}\right], \quad (3.1)$$

where ω is the angular frequency of the microwave probing signal and ν is the average frequency of collisions in which an electron loses its total momentum.

In practice most microwave-probe methods are restricted to electron densities considerably below the plasma-frequency limit, $N=\omega^2m\epsilon_0/e^2$. The dielectric post method is mainly limited by skin effect[2,4] which does not become important in this case until the electron density approaches $10^{13}/\mathrm{cm}^3$. The plasma-frequency limit corresponds to $N\sim 10^{11}/\mathrm{cm}^3$.

As Margenau[5] has stated, Eq. (3.1) fails to take into account the distribution of electron velocities and therefore cannot give a correct average for all electrons. Margenau[6,7] has derived expressions for the dielectric constant of an ionized gas for various forms of electron-velocity distribution function and Margenau and Stillinger[8] have shown that Eq. (3.1) is a satisfactory approximation to the results for the Maxwellian distribution function.

[4] J. M. Anderson, Rev. Sci. Instr. **32**, 975 (1961).

[5] H. Margenau, Phys. Rev. **69**, 508 (1946).
[6] H. Margenau, Phys. Rev. **109**, 6 (1958).
[7] E. A. Desloge, S. W. Matthysse, and H. Margenau, Phys. Rev. **112**, 1437 (1958).
[8] H. Margenau and D. Stillinger, J. Appl. Phys. **30**, 1385 (1959).

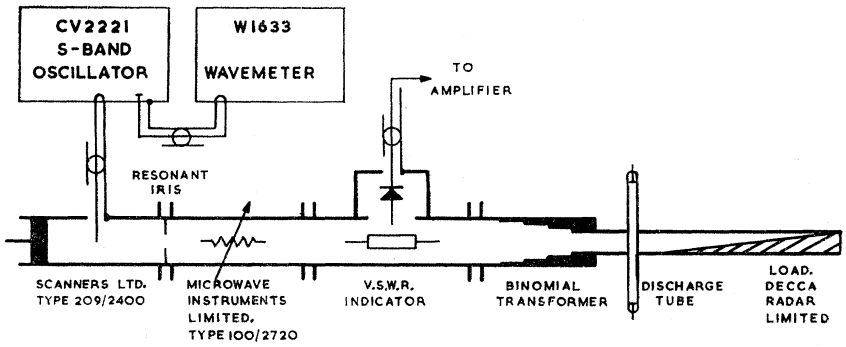

FIG. 2. The microwave system.

It can be shown[9] that for the range $1<(\omega/\nu)<10$ the error introduced by the use of Eq. (3.1) should not exceed 10% for the electron density and 20 to 30% for the collision frequency, even for extreme forms of the velocity distribution function.

The value of (ν/ω) can therefore be calculated directly from the ratio $\epsilon_r''/(1-\epsilon_r')$ and N can then be obtained from ϵ_r' or ϵ_r''.

4. EXPERIMENTAL PROCEDURE

A diagram of the microwave system is given in Fig. 2. The discharge tube was mounted across a section of waveguide with a height of 1 cm, matched to the standard waveguide dimensions by a 1:3:3:1 binomial transformer.[10] The oscillator output power was approximately 100 mW and the microwave signal in the discharge tube section was 30 dB below this level. At this power level the voltage standing-wave ratio (v.s.w.r.) probe had a square-law characteristic. The waveguide flanges were carefully aligned to avoid introducing unwanted discontinuities and the v.s.w.r. measured in the waveguide system was 0.98 before the holes for the discharge tube were machined.

Measurements were made for a post of known dielectric constant to verify the reliability of the results given in Fig. 1 and to confirm that the discharge tube itself could be considered as an additional constant admittance in parallel with the ionized gas. Tests were also made which showed that leakage of microwave power along the axis of the discharge tube was negligible for electron densities less than $10^{13}/\text{cm}^3$, and that the microwave probing signal did not significantly affect the discharge, even during the afterglow period. For the geometry and microwave frequency used, the lowest electron density which could be measured was in the region of $(10^{10}-10^{11})/\text{cm}^3$.

The gas discharge tubes were made from precision-bore Pyrex tube, 7.5-mm internal diameter, externally ground to 9-mm diameter. An electrode spacing of 20 cm was found to be suitable for discharges in helium at 5 to 15 mm Hg pressure and molybdenum or tungsten electrodes were used. The glass and electrodes were carefully outgassed by heating at 400°C and further cleaned by flushing with helium and running a glow discharge in the tube. All tubes were filled with helium of spectroscopic purity and sealed off at the required pressure: Barium getters were included to absorb impurities released after sealing off. The only impurities which could be detected spectrographically were molybdenum or tungsten sputtered from the cathode.

In order to study the behavior of a pulsed discharge using this dielectric post method, it is necessary to measure the v.s.w.r. in the waveguide as a function of time. The v.s.w.r. at any instant is a measure of the discharge admittance and it can be obtained by recording the probe output voltage waveform for a number of probe positions so that a permanent record of the time-varying v.s.w.r. pattern is obtained. In practice, the probe output signal required amplification before it could be displayed on an oscilloscope, so in order to avoid the difficulties associated with a high-gain dc amplifier the microwave oscillator was pulsed on for 1 msec when the discharge tube was pulsed. An amplifier with a bandwidth of 1 cps–1 Mc/sec was then sufficient to record changes in v.s.w.r. which occurred in a time of the order of microseconds, while the error due to removal of the dc component of the probe signal

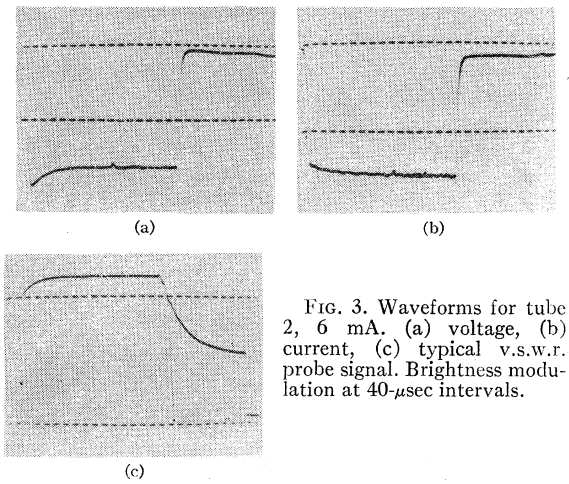

FIG. 3. Waveforms for tube 2, 6 mA. (a) voltage, (b) current, (c) typical v.s.w.r. probe signal. Brightness modulation at 40-μsec intervals.

[9] C. W. Davidson, Ph.D. thesis, University of Edinburgh, 1960 (unpublished).

[10] G. C. Southworth, *Principles and Application of Waveguide Transmission* (D. Van Nostrand Company, Inc., New York, 1950), p. 269.

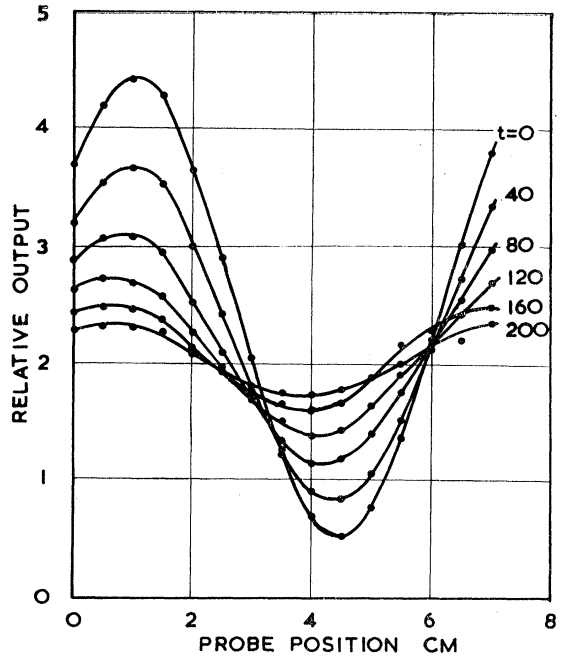

FIG. 4. Time-resolved v.s.w.r. pattern for the afterglow period. (t = time in microseconds measured from the end of the current pulse).

was negligible at the pulse repetition frequency of 12.5 pulses/sec.

The microwave oscillator was triggered directly from a pulse generator while the discharge tube was pulsed after a delay of a few microseconds, so that the microwave signal had reached a steady state before measurements were made. The discharge tube was fed with rectangular current pulses 640 μsec long from a generator with a dynamic impedance of the order of 1 MΩ. A dc maintaining current of 250 μA was used to ensure consistent timing of the current pulses. Typical discharge tube voltage and current waveforms and probe output signal are shown in Fig. 3.

The amplified probe signal was displayed on an oscilloscope and recorded at 5-mm intervals along the slotted waveguide section for each set of operating conditions and the v.s.w.r. plotted as a function of time, as shown in Fig. 4, for the afterglow period. The time variation in discharge parameters was then calculated using a standard microwave admittance chart and the results of Eqs. (2.1) and (3.1).

It is estimated that the values of electron density obtained by this technique may be in error by 20%. The values of collision frequency are less accurate, as the electron velocity distribution function was unknown, but they will at least be correct in order of magnitude.

5. RESULTS

Measurements have been made with four discharge tubes for helium pressures in the range 5 to 15 mm Hg. Details of these tubes were as follows:

Tube 1, helium at 5 mm Hg pressure, molybdenum electrodes;
Tube 2, helium at 10 mm Hg pressure, molybdenum electrodes;
Tube 3, helium at 15 mm Hg pressure, molybdenum electrodes;
Tube 4, helium at 10 mm Hg pressure, tungsten electrodes.

Under typical conditions the negative glow extended for about 1 cm from the cathode with the maintaining current alone, while under pulsed conditions it extended for about 5 cm and the positive column was about 12 cm in length, depending upon the gas pressure and current. A few diffuse stationary striations were visible at the head of the positive column and moving striations of the type observed by Donahue and Dieke[11] were present. These moving striations tended to be unstable near the anode end of the tube. The period of the oscillations in light intensity produced by the moving striations was roughly proportional to gas pressure and the phase advanced towards the anode. At 10 mm Hg pressure the corresponding striation velocity was approximately 400 m/sec.

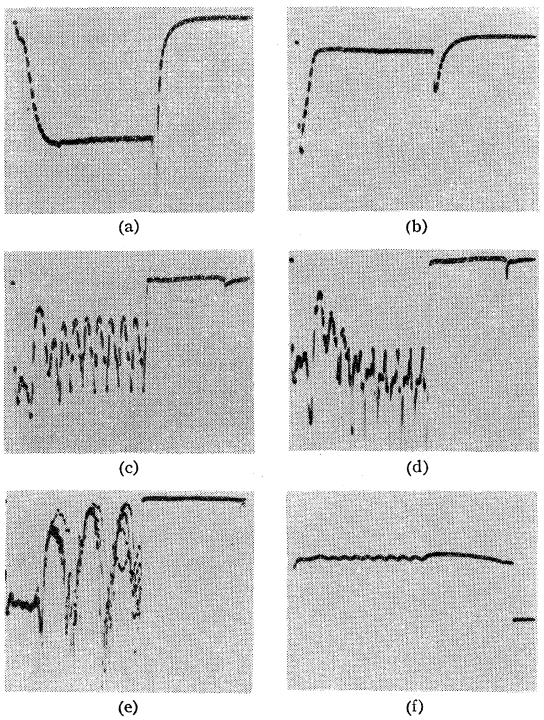

FIG. 5. Variation of total light intensity along the axis of a pulsed glow discharge in helium. Tube 2, 10 mA. (a) $x=2$ cm, negative glow (gain reduced $\times 10$); (b) $x=8$ cm, dark space; (c) $x=9.7$ cm, first striation; (d) $x=10$ cm, first minimum; (e) $x=19$ cm, positive column; (f) Corresponding v.s.w.r. probe signal for the positive column. Brightness modulation at 40-μsec intervals.

[11] T. Donahue and G. H. Dieke, Phys. Rev. **81**, 248 (1951).

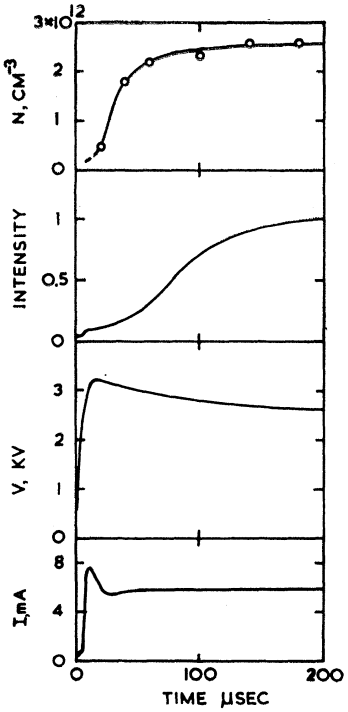

FIG. 6. Discharge behavior at the onset of the current pulse. Tube 4, $x=2$ cm.

The total light intensity was studied using a double slit system and photomultiplier tube to sample the intensity over a 1/8-in. length of the tube. Results obtained in this way are shown in Fig. 5. (x=distance from the cathode in cm).

The electron density in the positive column was too low to allow accurate measurements to be made, but the v.s.w.r. probe signal shown in Fig. 5(f) indicates that the moving striations were accompanied by large fluctuations in electron density.

The form of the electron density increase in the negative glow region at the onset of the current pulse is shown in Fig. 6 along with voltage, current, and light intensity wave forms. The axial variation in electron density is shown in Fig. 7. The axial variation in collision frequency was less marked, but there was a maximum near the cathode.

Figure 8 shows electron-density and collision-frequency variation during the recombination period following the end of the current pulse. The corresponding light intensity plot is shown on a logarithmic scale in Fig. 9.

Measurements of the intensity of the individual spectral lines in the visible region were made using a small grating-type spectrometer and photomultiplier tube. In the negative glow region the line intensities had the general form shown in Fig. 10(b) with a pronounced afterglow following the end of the current pulse. However, the 3 ^1P–2 ^1S line (5016 Å) decayed monotonically without the initial increase in intensity [Fig. 10(c)] and increased more rapidly at the onset of the current pulse. Because of the high noise level, accurate measurement of the individual line intensities was not attempted, but the weakest lines during the current pulse tended to show the largest percentage intensity increase in the afterglow.

In the positive column all spectral lines had the form shown in Fig. 5(c) and no significant afterglow could be detected.

6. DISCUSSION

In these experiments current pulses were superimposed on a small steady maintaining current in a glow discharge. The maximum rate of rise of discharge tube voltage (Fig. 6) was limited by the bandwidth of the current generator. Since the discharge tube current is controlled by the increase of electron density and drift velocity, the rise in discharge current is delayed with respect to the applied voltage; the delay increases with gas pressure, corresponding to the reduction in X/p, where X is the electric field strength and p the gas pressure. The cathode fall of potential will be high and the electron density will not reach its final value until emission processes at the cathode reach a steady state. The delay will therefore be controlled by the relatively heavy positive ions.

Chanin and Biondi[12] give a value of approximately 10 cm^2/V sec for the mobility of positive ions in helium. Assuming a cathode dark space of the order of 0.5 cm across and an electric field strength $X \sim 10^3$ V/cm positive ions would take about 50 μsec to cross the dark space. In fact 100 to 200 μsec are required before the discharge becomes stable. The light intensity depends upon both electron density and electron temperature and therefore increases less rapidly than the electron density.

Following the end of the current pulse, the electron density is much greater than required to maintain the discharge and the tube voltage falls to a few hundred volts for about 1 msec while recombination occurs. The electron temperature variation corresponding to the

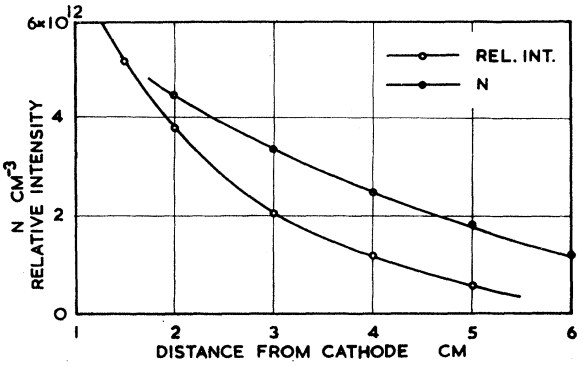

FIG. 7. Typical axial variation of electron density and light intensity.

[12] L. M. Chanin and M. A. Biondi, Phys. Rev. 94, 910 (1954).

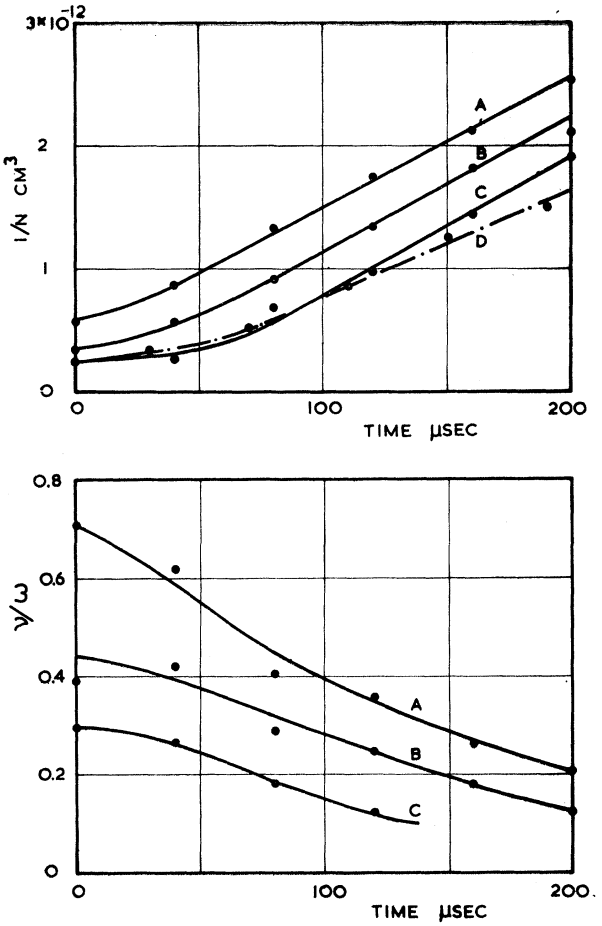

FIG. 8. Electron density and collision frequency during the afterglow period. (Time measured from the end of the current pulse.) (a) tube 3, 4 mA. (b) tube 1, 6 mA. (c) tube 2, 6 mA. (d) tube 4, 6 mA.

results of Fig. 8 has been calculated using the equations given by Margenau.[5] During the current pulse values of approximately 5×10^3 °K were obtained, falling to less than 10^3 °K 100 μsec after the end of the pulse. The initial values are much lower than might be expected, although it is known that the electron-velocity distribution function in the negative glow region is not normally Maxwellian,[13] but it should tend to become Maxwellian during the recombination period. Ambipolar diffusion may be present, in addition to recombination, following the end of the current pulse, but the diffusion time constant[14] in these experiments was of the order of 1 msec so that recombination was the main electron loss process during the first few hundred microseconds. This is confirmed by the constant slope of the inverse electron-density plots as a function of pressure (Fig. 8) and by the $1/t^2$ variation of the light intensity which exists 80–100 μsec after the end of the current pulse (Fig. 9). The values of recombination coefficient for helium obtained from Fig. 8 are $\alpha_{He}=1.1\times10^{-8}$ cm³/ion sec and $\alpha_{He}=8.8\times10^{-9}$ cm³/ion sec. The difference may be partly due to the presence of the cathode material as an impurity. These values are in good agreement with values measured at 10 Gc/sec by other microwave methods.[15,16]

The large increase in light intensity during the early stages of recombination can be explained by assuming that α is a sensitive function of electron energy. Phelps *et al.*[17] state that in helium the electron temperature falls to within 10% of the gas temperature in a few microseconds at these pressures, and Chen *et al.*[16] have shown that α varies as $T_e^{-\frac{3}{2}}$, so that the recombination rate would increase rapidly following the removal of excitation.

The apparently anomalous behavior of the 5016 Å line, corresponding to the $3\,^1P-2\,^1S$ transition[18] may be due to reabsorption of the line by the large metastable population. Gabriel and Heddle[19] give the relative probabilities for the $2\,^1P-1\,^1S$ and $2\,^1P-2\,^1S$ transitions as 1.79×10^9/sec and 1.97×10^6/sec and for the $3\,^1P-1\,^1S$ and $3\,^1P-2\,^1S$ transitions as 5.71×10^8/sec and 1.34×10^7/sec, respectively. Thus, radiation corresponding to transitions to the $2\,^1S$ metastable state may be reabsorbed by a metastable atom with a high probability that the atom will then return to the ground

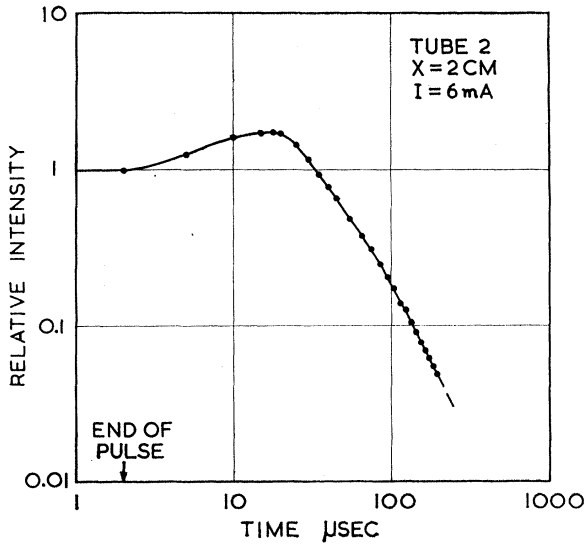

FIG. 9. Total light intensity following the end of the current pulse.

[13] D. H. Pringle and W. E. J. Farvis, Proc. Phys. Soc. (London) **B67**, 836 (1955).
[14] L. Goldstein, *Advances in Electronics and Electron Physics* (Academic Press Inc., New York, 1955), Vol. 7.
[15] R. A. Johnson, B. T. McClure, and R. B. Holt, Phys. Rev. **80**, 376 (1950).
[16] C. L. Chen, C. C. Leiby, and L. Goldstein, Phys. Rev. **121**, 1391 (1961).
[17] A. V. Phelps, O. T. Fundingsland, and S. C. Brown, Phys. Rev. **84**, 559 (1951).
[18] G. Herzberg, *Atomic Spectra and Atomic Structure* (Dover Publications, Inc., New York, 1944), p. 65.
[19] A. Gabriel and D. Heddle, Proc. Roy. Soc. (London) **A258**, 124 (1960).

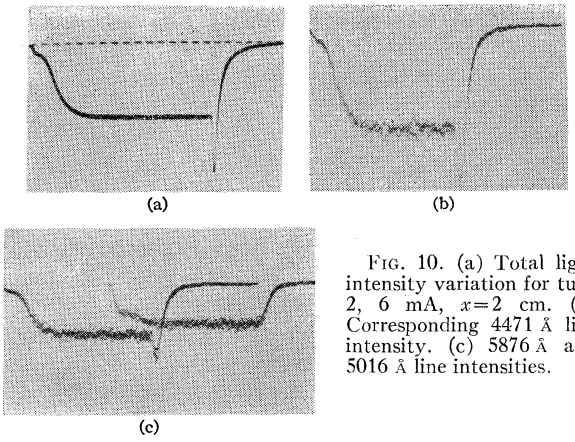

FIG. 10. (a) Total light intensity variation for tube 2, 6 mA, $x=2$ cm. (b) Corresponding 4471 Å line intensity. (c) 5876 Å and 5016 Å line intensities.

state; leading to an increase in the intensity of the corresponding lines. No similar effect could be observed in the case of the $2\,^3S$ metastables, since transitions to the singlet states are forbidden and are extremely weak in practice. In fact, the triplets show an afterglow effect similar to the normal singlet lines.

The rapid increase in the 5016 Å line intensity at the onset of the current pulse can also be explained on this basis, since the increased number of transitions would rapidly reach equilibrium with the metastable population, so that no further increase in line intensity could be observed.

The addition of air as an impurity, which would destroy metastables due to the Penning effect, removed all trace of the initial increase in light intensity during the afterglow.

Johnson[15] and Anderson[20] have made measurements of the recombination spectra of discharges in helium and have found the band spectra of He_2^+ to be prominent. In these experiments, however, only the line spectrum of atomic helium was observed. This may be due to a different level of excitation.

Having obtained the electron density from the microwave measurements it is possible to estimate the electric field strength. For the negative glow region the electron density is approximately $10^{12}/cm^2$ and the current density approximately 14 mA/cm^2 for a 6 mA pulse. The electron drift velocity must therefore be about 10^5 cm/sec. Bradbury and Nielsen[21] give the corresponding $X/p\sim 0.1$ V/cm-mm Hg, so that the electric field is of the order of 1 V/cm. In the positive column where the electron density is one or two orders of magnitude lower the value would be 10 to 100 V/cm.

ACKNOWLEDGMENTS

This work was supported by an Admiralty (CVD) contract and their assistance is gratefully acknowledged.

[20] J. M. Anderson, *Proceedings of the Fifth International Conference on Ionization Phenomena in Gases*, Munich, 1961 (unpublished).

[21] L. B. Loeb, *Basic Processes of Gaseous Electronics* (University of California Press, Berkeley, 1955), p. 232.

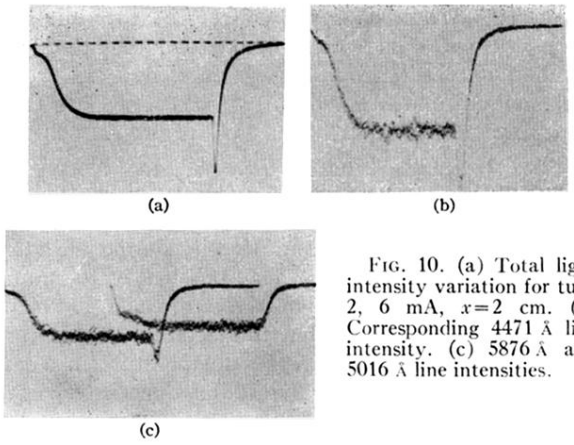

FIG. 10. (a) Total light intensity variation for tube 2, 6 mA, $x=2$ cm. (b) Corresponding 4471 Å line intensity. (c) 5876 Å and 5016 Å line intensities.

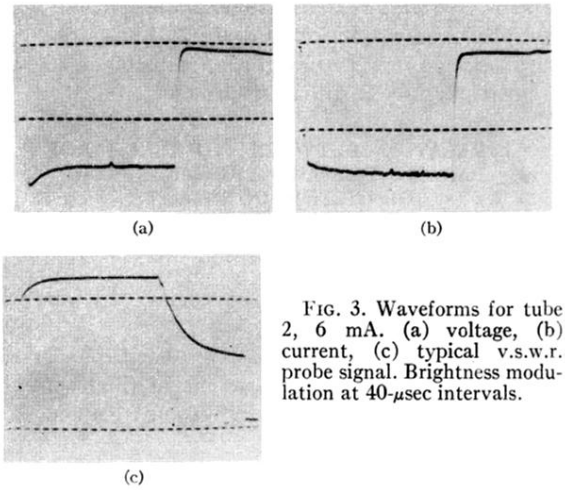

FIG. 3. Waveforms for tube 2, 6 mA. (a) voltage, (b) current, (c) typical v.s.w.r. probe signal. Brightness modulation at 40-μsec intervals.

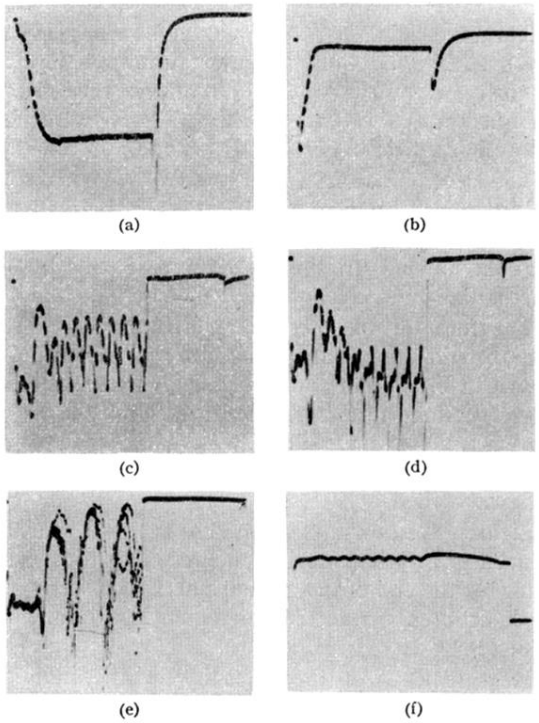

FIG. 5. Variation of total light intensity along the axis of a pulsed glow discharge in helium. Tube 2, 10 mA. (a) $x=2$ cm, negative glow (gain reduced $\times 10$); (b) $x=8$ cm, dark space; (c) $x=9.7$ cm, first striation; (d) $x=10$ cm, first minimum; (e) $x=19$ cm, positive column; (f) Corresponding v.s.w.r. probe signal for the positive column. Brightness modulation at 40-μsec intervals.